NIH Public Access
Author Manuscript
Mol Pharm. Author manuscript; available in PMC 2014 May 23.

Published in final edited form as:
Mol Pharm. 2013 October 7; 10(10): 3655–3664. doi:10.1021/mp400130w.

Preclinical Evaluation of the Novel Monoclonal Antibody H6-11 for Prostate Cancer Imaging

Hongjun Jin, **Mai Xu**, **Prashanth K. Padakanti**, **Yongjian Liu**, **Suzanne Lapi**, and **Zhude Tu***
Department of Radiology, Washington University School of Medicine, 510 S. Kingshighway Boulevard, St. Louis, Missouri 63110, United States

Abstract

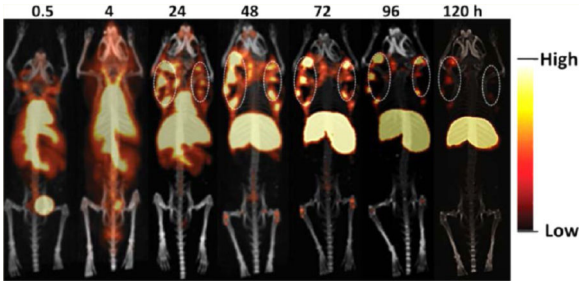

The biological properties of the novel monoclonal antibody (mAb) H6-11 and its potential utility for oncological imaging studies were evaluated using *in vitro* and *in vivo* assays. Immunoreactivity of H6-11 to the human prostate cancer PC-3 cell line and solid tumor xenografts was initially demonstrated using immunofluorescence staining; the specificity of H6-11 for prostate cancer was further evaluated using a commercial array of human prostate cancer and normal tissue samples (n = 49) in which H6-11 detected 95% of prostate adenocarcinomas. The K_d value of 61.7 ± 30 nM was determined using ^{125}I-labeled H6-11. Glycosylation analysis suggested the antigenic epitope of the glycan is an O-linked β-*N*-acetylglucoside (*O*-GlcNAc) group. Imaging studies of PC-3 tumor-bearing mice were performed using both optical imaging with NIR fluorescent dye-labeled H6-11 and microPET imaging with ^{89}Zr-labeled H6-11. These *in vivo* studies revealed that the labeled probes accumulated in PC-3 tumors 48–72 h postinjection, although significant retention in liver was also observed. By 120 h postinjection, the tumors were still evident, although the liver showed significant clearance. These studies suggest that the mAb H6-11 may be a useful tool to detect prostate cancer *in vitro* and *in vivo*.

© 2013 American Chemical Society

***Corresponding Author**. Department of Radiology, Washington University School of Medicine, Campus Box 8225, 510 S. Kingshighway Blvd., St. Louis, MO 63110, USA. Tel: 1-314-362-8487. Fax: 1-314-362-8555. tuz@mir.wustl.edu.

ASSOCIATED CONTENT

Supporting Information

Immunostaining data, immunoreactivity data, autoradiogrrarphic study results, and amino acid sequence for the CDRs region of H-11 hybridoma cell line. This material is available free of charge via the Internet at http://pubs.acs.org.

Notes

The authors declare no competing financial interest.

NIH-PA Author Manuscript
NIH-PA Author Manuscript
NIH-PA Author Manuscript

NIH-PA Author Manuscript

NIH-PA Author Manuscript

NIH-PA Author Manuscript

Keywords

prostate cancer; mAb; O-GlcNAc; positron emission tomography (PET); PC-3; glycosylation; tumor-associated carbohydrate antigens (TACA)

INTRODUCTION

Cancer cells can demonstrate unusual patterns of glycosylation which result in high levels of specific tumor-associated carbohydrate antigens (TACA). There is considerable evidence that some of these residues are associated with breast cancer,[1,2] prostate cancer,[3–7] and other cancers.[8–10] Several carbohydrate antigens, including the TF and Tn antigens,[3,11,12] sialyl Lewis^X,[4,13] and Globo-H[14–16] have been reported to be important in cancer development and progression. These structural changes can alter cellular function including a cancer cell's adhesive properties and potential to invade and metastasize. A growing body of evidence indicates that proteins synthesized by early stage tumors are subject to post-translational modifications including altered glycosylation pathways which have been associated with immune response.[9,10,17,18] Because glycosylation of cancer-related biomarkers can be determined using specific antibodies, we hypothesized that antibodies against specific glycosylation would be valuable tools for *in vivo* cancer detection.

The potential utility of circulating glycoprotein markers such as CA-125 and human epididymis protein (HE)4 to identify and monitor the progression of prostate and other cancers have been extensively investigated in the clinic.[8,19] Such markers have been particularly useful in monitoring therapeutic response and for detecting tumor recurrence post-treatment. Although studies have revealed that CA-125 is not tumor specific,[20,21] the strategy of combining multiple tumor markers found in serum has been shown to facilitate the detection of early stage tumors and accurately identify tumor recurrence.[22,23] Unfortunately, serum markers cannot be used to determine tumor volume or location, which is critical information in the clinical management of cancer patients. Antibodies which recognize glycoprotein markers have been used for preclincal positron emission tomography (PET) studies as well as clinical studies with single photon emission computed tomography (SPECT) probes and show selective binding to tumors over healthy tissues.[24–26] In the current study, the novel mAb H6-11 originally identified using the human colon adenocarcinoma cell line, NSY42129,[27] was evaluated against a panel of 40 human prostate carcinoma samples, 8 samples of normal prostate tissue, and 1 hepatic carcinoma sample; the expression of mAb H6-11 binding epitope in the PC-3 prostate cancer cell line was also examined. We found that mAb H6-11 recognizes a β-*N*-acetylglucoside group. We further explored the feasibility of imaging solid tumor xenografts of PC-3 in athymic nu/nu mice by optical imaging and microPET. In these studies, mAb H6-11 distinguished the tumor from surrounding normal tissue. Thus, a glycoprotein-recognizing antibody like mAb H6-11 may be valuable for prostate cancer imaging.

NIH-PA Author Manuscript

NIH-PA Author Manuscript

NIH-PA Author Manuscript

EXPERIMENTAL SECTION

Cell Lines and Cell Culture

Human colon adenoma cell line NSY42129 was cultured in RPMI 1640 supplemented with 10% fetal calf serum (FCS) (Hyclone Laboratory Inc., Logan, Utah), 50 units/mL sodium penicillin (BioWhittaker Inc., Walkersville, Maryland), and 50 μg/mL streptomycin sulfate (BioWhittaker). Myeloma cells (P3/x63·Ag8) used as a fusion partner were maintained in Iscove's modified Dulbecco's medium supplemented with 20% fetal bovine serum (FBS) (Hyclone), 50 units/mL sodium penicillin, 50 μg/mL streptomycin sulfate, 4 mmol/L L-glutamine (BioWhittaker), 1 mM sodium pyruvate (BioWhittaker), and 0.0001% β-mercaptoethanol (Sigma-Aldrich Inc., St. Louis, MO). The human prostate cancer PC-3 cell line was cultured in RPMI 1640 medium supplemented with 10% FCS, 50 units/mL sodium penicillin, 50 units/mL streptomycin sulfate, and 2 mM L-glutamine. MCF-7 human breast cancer cells were maintained in DMEM supplemented with 10% FCS, 50 units/mL sodium penicillin, and 50 units/mL streptomycin sulfate. H6-11 hybridoma cells used for antibody production (H-20, obtained through the Washington University School of Medicine Hybridoma Center) were cultured in Iscove's modified Dulbecco's medium supplemented with 20% fetal bovine serum, 50 units/mL sodium penicillin, 50 units/mL streptomycin sulfate, 4 mM L-glutamine, 1 mM sodium pyruvate, and 0.0001% β-mercaptoethanol. All cells were cultured in a humidified incubator at 37 °C with 5% CO_2. For cDNA sequencing, the frozen H6-11 hybridoma cell line was sent to GenScript Inc. (Piscataway, New Jersey). The consensus complementarity-determining regions (CDR) DNA sequencing was successfully achieved through 10 codon RT-PCR following standard procedures.

Generation of mAb H6-11

All animal procedures were performed according to protocols approved by the Animal Studies Committee of the Washington University School of Medicine in accordance with the Guide for the Care and Use of Laboratory Animals. As previously described,[9,18] 6-week-old female BALB/c mice were injected i.p. with Titermax Gold adjuvant (25 μL; Sigma-Aldrich) and NSY42129 cells (1×10^6) once a week for 4 weeks. Three days before euthanasia, each mouse was boosted with the same doses of adjuvant and tumor cells. Spleen cells from mice with a serum titer >4,000 were used for fusion. A hybridoma library was established by fusion of spleen cells from the immunized BALB/c mice and myeloma cells (P3/x63·Ag8) at a 5:1 ratio with polyethylene glycol (PEG)-1500 (Sigma-Aldrich) following standard procedures.[28,29] H6-11 mAb was purified from the supernatant of the H6-11 hybridoma cell line using a NAb Protein A/G Spin Column (Thermo Scientific, Rockford, IL) according to the manufacturer's instructions. The concentration of the purified antibody was quantified by measuring the absorbance at 280 nm on a UV–vis Nanodrop spectrophotometer (Nanodrop Technologies Inc., Wilmington, DE).

Immunofluorescence Staining of PC-3 Cells

An immunofluorescence staining assay was used as previously reported to examine the expression of the mAb H6-11 binding antigen in PC-3 prostate cancer cells with or without fixation.[9,18,30] To stain the PC-3 cells, 50 μL of mAb H6-11 at a concentration of 5 μg/mL in PBS was added to the Lab-Tek chamber slide and incubated for 40 min at 37 °C. The

NIH-PA Author Manuscript

NIH-PA Author Manuscript

NIH-PA Author Manuscript

slide was washed 3× with PBS, then 50 μL of 1,000× diluted FITC-conjugated goat antimouse IgG in PBS (Jackson Immuno Research Laboratory Inc., West Grove, PA) was added to each well. The slides were incubated for another 40 min at room temperature. Slides were washed with PBS and observed under a confocal fluorescence microscope FV1000 (Olympus America, Center Valley, PA). Slides containing 20 μm sections of PC-3 solid tumors and surrounding normal muscle from xenografts implants were also used for immunofluorescence staining using procedures similar to those for PC-3 cell staining using H6-11 as the primary antibody as described above.

Immunohistochemical Staining of a Tissue Array of Prostate Cancer and Normal Tissue

To confirm the potential clinical utility of mAb H6-11 in prostate cancer, its specificity was evaluated using an array of human prostate cancer and normal tissue. Slide-mounted histologic samples of 40 human prostate carcinoma specimens, 8 samples of normal prostate tissue, and 1 hepatic carcinoma (US Biomax Inc. Rockville, MD) were deparaffinized in xylene and rehydrated through gradient alcohols as described previously.[9,18,30] The slides were further incubated with mAb H6-11 as the primary antibody at a concentration of 5 μg/mL overnight at 4 °C. Avidin–Biotin Complex Detection System (Vector Laboratory) was then used for chromogenic slide development following standard procedures.[9,18,30] The results were classified into the following categories based on staining intensity and percentage: grade 0 or no staining (−); grade 1 or modest staining (+); grade 2 or positive staining (++); grade 3 or strong positive staining (+++).

^{125}I-Labeling of H6-11

Iodogen solid-phase iodination reagent (Thermo Fisher Pierce Scientific Inc., Rockford, IL) was then used for ^{125}I-labeling of H6-11 following the manufacturer's instructions. Briefly, 0.1–0.2 mg of the purified mAb H6-11 in 0.1 mL of 100 mM, pH 7.4, PBS was treated with 1.0 mCi of [^{125}I]NaI (MP Biomedicals, LLC, Santana, CA) in a reaction vessel which had been plated with the Iodogen reagent. Unlabeled small molecules were removed from the radiolabeled product by passing the reaction mixture through a desalting column (Thermo Fisher Pierce Scientific Inc., Rockford, IL). Labeling efficiency was calculated by measuring the radioactivity of bound IgG as a percentage of total radioactivity. The radiochemical yield was 30–40%. To further confirm IgG labeling, radiolabeled antibody samples were loaded onto SDS–PAGE, and the gel was directly developed on the FLA7000 imaging system (GE Healthcare Biosciences, Piscataway, NJ). The light chain and heavy chain of IgG were both visualized using this autoradiography system.

In Vitro Autoradiography

The immunoreactivity of mAb H6-11 to PC-3 prostate cancer xenografts was evaluated through *in vitro* autoradiography studies using the radio-iodinated antibody. Slides containing 20 μm sections from snap-frozen PC-3 tumors were incubated with ^{125}I-labeled H6-11 (1 μCi/mL) in PBS at room temperature for 2 h. After washing three times with PBS/0.01% Tween-20, the slides were air-dried. Dry slides were loaded into the Fuji film phosphor imager film cassette for 12 h at 4 °C in the dark before exposing to a phosphorimager screen and capturing with a Fujifilm FLA-7000 imaging system (GE

NIH-PA Author Manuscript

NIH-PA Author Manuscript

NIH-PA Author Manuscript

Healthcare). Photostimulated luminescence (PSL) was quantitated with Fuji Image Gauge software.

Characterization of ^{125}I-Labeled H6-11 through Binding Assays

Immunoreactivity of mAb H6-11 was determined by incubating the radioiodinated antibody (≈100,000 cpm) with PC-3 cells (seeded in a 96-well plate at 1×10^5cells/well in PBS/1% FBS). Serial dilutions of ^{125}I-labeled H6-11 (1–133 nM) were added and allowed to incubate for 1 h before the samples were washed with PBS/1% FBS. Three hundred microliters of scintillation cocktail (RPI Corp, Prospect, IL) was added to each well, and the radioactivity of bound antibody was measured with a 1450 MicroBeta Trilux liquid scintillation counter (PerkinElmer Life Health Sciences., Shelton CT). The plot of the bound radioactivity versus the concentration of antibody was fitted to the saturation binding curve using Prism (GraphPad Software Inc., La Jolla, CA), which was used to calculate the binding dissociation constant (K_d) and B_{max}.

Antigen Epitope Characterization by Immunostaining

To characterize the epitope of mAb H6-11, deglycosylation experiments were conducted as previously described[10,17] with some modifications. Briefly, PC-3 or MCF-7 cells were seeded (1×10^5/well) in a 96-well plate, incubated at 37 °C for 48 h, and fixed with 10% neutral buffered formalin for 30 min. After washing twice with PBS and adding 100 μL of a range of concentrations (in triplicate) of sodium periodate (1, 5, 10, and 20 mmol/L in pH 4.5 sodium acetate buffer), trypsin (0.5–2.0 mg/mL in PBS), or deglycosylation reagents (Prozyme Inc., Hayward, CA) into each well of the 96-well plate, the plates were incubated at 37 °C for 2 h for sodium periodate, 1 h for trypsin, and 24 h for the plate treated with deglycosylation reagents. After washing the fixed cells with PBS containing 10% FBS, mAb H6-11 was added to each well at a concentration of 10 μg/mL; this was followed by incubation for 1 h at 37 °C. The secondary antibody, FITC-conjugated goat antimouse, was incubated with the cells in the plates for 45 min. The 96-well plates were read with a Synergy HT Multi-Detection microplate reader (BioTek US, Winooski, VT).

NIR Labeling and *in Vivo* Optical Imaging of the PC-3 Xenograft

In order to evaluate the potential application of H6-11 as a molecular imaging probe, *in vivo* optical imaging experiments were performed using the mAb H6-11 conjugated with IRDye 800CW. The conjugation of protein and NIR dye was done by using the IRDye 800 Protein Labeling Kit (LI-COR Biosciences, Lincoln, Nebraska) as described previously.[9] Mature male athymic nu/nu mice were subcutaneously implanted with PC-3 tumor cells as previously described.[31,32] Tumor-bearing mice were anesthetized with 2% isoflurane/oxygen and placed on the scanner bed for noninvasive optical imaging of the ventral surface. Then, 100 μg of IRDye 800CW-labeled mAb H6-11 in 100 μL of PBS solution was administered by intravenous (i.v.) tail vein injection, and static images were acquired using the Xenogen IVIS-200 optical imager at the indicated time points (0, 24, 48, 72, 96, and 120 h). Imaging data were collected and analyzed by using Living Imaging 3.6 software (Caliper Life Sciences, Alameda, CA) according to the manufacturer's instructions.

NIH-PA Author Manuscript

NIH-PA Author Manuscript

NIH-PA Author Manuscript

^{89}Zr Production and Antibody Labeling

Because of promising results in the optical imaging study, mAb H6-11 was radiolabeled with ^{89}Zr for microPET imaging. ^{89}Zr was produced via the ^{89}Y(p,n) ^{89}Zr nuclear reaction using a CS-15 cyclotron (Cyclotron Corporation, Berkeley, CA) and separated via ion exchange at the Washington University Cyclotron Facility with a specific activity of 8.1 to15.4 GBq/mol. The labeling and purification procedure followed previously published methods.[33,34] Briefly, 50 μL of purified mAb H6-11 (5 mg/mL) was incubated with the bifunctional chelator, *p*-isothiocyanatobenzyl-desferrioxamine (*p*-SCN-Bz-DFO) (Macrocyclics Inc., Dallas, TX), in 0.1 M $NaHCO_3$ buffer (pH 9.0) at 4 °C overnight. The product, *p*-SCN-Bz-DFO-H6-11, was purified via Zeba Spin desalting columns (Pierce Biotechnology, Rockford, IL). ^{89}Zr (in 1.0 M oxalic acid) was then complexed with the *p*-SCN-Bz-DFO-H6-11 at a ratio of 222 MBq/mg (6 mCi/mg) of antibody in 0.5 M HEPES buffer at pH 7.0 at 37 °C for 1 h with constant agitation. ^{89}Zr-*p*-SCN-Bz-DFO-H6-11 was purified with a Zeba Spin desalting column, and the radiochemical purity was determined by radio-TLC (silica) using a mobile phase of 50 mM diethylenetriamine pentaacetic acid (DTPA) and confirmed with SDS–PAGE autoradiography. The specific activity was ~1 μCi/μg.

MicroPET Imaging

PC-3 tumors were implanted subcutaneously in male athymic nu/nu mice as previously described.[31,32] For microPET imaging using an Inveon MicroPET/CT scanner (Siemens Inc., Knoxville, TN), mice were anesthetized with 2% isoflurane/oxygen, positioned side-by-side in a custom bed, and tail vein catheters were placed. Tumor-bearing mice (n = 2) were injected with 150 μCi/100 μL ^{89}Zr-labeled H6-11 in saline. Initial 30 min dynamic images was acquired; subsequent 30 min static images were obtained at 4, 24, 48, 72, 96, and 120 h postinjection. PET images were coregistered with CT using image display software (Inveon Research Workplace, Siemens). Acquisition time for CT data was 10 min (1 bed position), and images were reconstructed using a filtered back projection reconstruction algorithm and displayed using the ASIPro VM software package, version 4.0 (Siemens Medical Solutions USA, Inc.).

RESULTS

Immunohistochemical Staining of a Tissue Array of Prostate Cancer and Normal Tissue

We previously screened other antibodies from our hybridoma library; several of those antibodies showed tumor specificity and potential for *in vivo* molecular imaging applications.[9,18,30] In this study, we first identified the novel mAb H6-11 by screening hybridoma libraries against human colon adenocarcinoma NSY42129 cells. We have previously reported that antibodies produced from mice immunized with this cell line also recognize surface antigens associated with other tumor types.[9,18,35] An array of 40 clinical human prostate cancer samples and 8 healthy human prostate tissues was used to determine the potential utility of the novel mAb H6-11 for the detection of prostate cancer. At first, we examined the reactivity of the antibody to human prostate cancer tissues to determine the sensitivity and accuracy of the epitope targeted by mAb H6-11. We found that 95% (38 of 40 adenocarcinoma cases) showed positive staining with H6-11. +, ++, and +++ were 20%,

NIH-PA Author Manuscript

NIH-PA Author Manuscript

NIH-PA Author Manuscript

45%, and 30%, respectively (Supporting Information, Tables S1 and S2). All of the prostate adenocarcinoma cases tested exhibited intense homogeneous staining; furthermore, the epitope recognized by H6-11 was expressed in all histologic grades of prostate cancers, as shown in Figure 1. In order to demonstrate specificity to tumor tissue, we also tested H6-11 with eight samples of normal prostate tissue. Our results showed that the mAb H6-11 binding was undetectable in fibromuscular stroma from healthy prostate glands, although weak positive staining was observed in the prostate epithelium (Figure 1 and Supporting Information, Table S1).

In Vitro Autoradiography with ^{125}I-H6-11

Radiolabeling of the novel mAb H6-11 with iodine-125 permitted further investigations. SDS–PAGE autoradiography of ^{125}I-labeled mAb H6-11 indicated the IgG molecule was iodinated on both the heavy chain and light chain (Supporting Information, Figure S1). Additional *in vitro* autoradiography studies were carried out with slides containing sectioned PC-3 tumor tissue and surrounding normal muscle from snap-frozen xenograft implants. ^{125}I-Labeled intact purified mouse IgG (mIgG) was used as the negative control, and glycolipid-specific antibody anti-Globo-H (MBr1)[14–16] (Enzo Life Sciences, Inc., Farmingdale, NY) was used as a positive control. ^{125}I-mIgG showed no detectable interaction with either the tumor or the muscle. ^{125}I-Globo-H reacted with both the tumor and muscle equally, while ^{125}I–H6-11 reacted strongly to PC-3 solid tumors but showed no binding to muscle. (Supporting Information, Figure S2) These results are consistent with the observation that in immunofluorescence staining, H6-11 preferentially bound to PC-3 prostate cancer cells from culture and solid tumors but showed little binding in the surrounding muscle and stroma (Figure 2).

Immunofluorescence Staining of PC-3 Cells

We performed immunofluorescence staining on cultured PC-3 cells with and without fixation to determine if mAb H6-11 antigen is expressed on the cell surface. Typical ring-like intense cell membrane staining was observed in cultured live PC-3 cells without fixation (Figure 2A). When PC-3 cells were fixed with 10% neutral buffered formalin, both the surface and cytoplasmic regions were intensively positive (Figure 2B). This suggests that the antigen to which mAb H6-11 binds may not only be located on the surface of the tumor cells but that it may also be present in the cytoplasm. As noted above, PC-3 solid tumor xenografts and normal muscle tissue which were snap-frozen and mounted on glass slides for incubation with mAb H6-11 and subsequent immunofluorescence staining also showed preferential and strong binding of the mAb to the tumor cells with little binding to the normal tissue (Figure 2C and D).

Characterization of ^{125}I-Labeled H6-11 through Binding Assays

To qualitatively study the binding of the novel mAb H6-11 to human prostate cancer,^{125}I-labeled H6-11 was used to measure the K_d and B_{max} with PC-3 cells. Variable concentrations of ^{125}I-labeled H6-11 were incubated with 1×10^5 PC-3 cells, then the unbound mAb was washed away, and the radioactivity which remained and was specifically bound to prostate cancer cells was measured on a liquid scintillation counter. On the basis of

NIH-PA Author Manuscript

NIH-PA Author Manuscript

NIH-PA Author Manuscript

radioactivity saturation binding curve fitting (Figure 3), the estimated B_{max} is 5651 ± 1320 cpm/1 × 10^5 cell, and specific binding K_d is 61.7 ± 30 nM. As a positive control, ^{125}I-labeled anti-Globo-H was similarly incubated with MCF-7 breast cancer cells, and specific binding was determined by the same procedure (Figure 3). Globo-H binding to MCF-7 cells showed B_{max} = 2536 ± 374 cpm/1 × 10^5 cell, and K_d = 26.9 ± 11 nM. The K_d for H6-11 and PC-3 is close to the K_d for Globo-H and MCF-7, indicating that mAb H6-11 has typical antigen–antibody binding to the PC-3 cells.

Antigen Epitope Characterization by Immunostaining

In general, most cell surface antigens with which antibodies react are glycoproteins or glycolipids, i.e., CA-199, CA-125, and Globo-H.[8,15,36,37] To further explore if the antigen of H6-11 is a glycoprotein or glycolipid, the epitope was characterized by deglycosylation experiments. We treated PC-3 and MCF-7 cells with different concentrations of trypsin, followed by radioactivity measurement using ^{125}I-labeled H6-11 and anti-Globo-H (MBr1), respectively. Because anti-Globo-H antibody recognizes the glycolipid antigens on the surface of MCF-7, the immunoreactivity was not affected by trypsin digestion (Supporting Information, Figure S3C). However, bound radioactivity significantly decreased with trypsin treatment of PC-3 cells (Supporting Information, Figure S3A). When the antigen on PC-3 was digested with trypsin, the polypeptide portion of the antigen was truncated; thus, the bound radioactivity decreased. This suggested that the H6-11 antigen contains a polypeptide that can be digested by trypsin. We also treated tumor cells with different concentrations of sodium periodate, followed by radioactivity measurement using ^{125}I-labeled H6-11 for PC-3 and ^{125}I-anti-Globo-H for MCF-7. Both experiments produced an increasing bound radioactivity suggesting that both antigens contain a glycan portion (Supporting Information, Figure S3B and D). Similar experiments have been reported previously;[10] periodate treatment uncovers the carbohydrate groups on the glycan, thus facilitating the antibody's access to the buried antigenic epitopes.

Glycoprotein Antigen Identification

To further identify the glycoprotein antigen, we lysed MCF-7 and PC-3 cell pellets, collected the membrane and cytoplasmic proteins, and then conducted western blot analysis using mAb H6-11 as a primary antibody. No distinct band was identified in the membrane-extracted proteins (data not shown), but proteins with an extremely high molecular weight lack mobility in SDS–PAGE. In contrast, soluble protein bands from cytoplasmic extractions of both MCF-7 and PC-3 cell pellets were identified (Figure 4A). Multiple bands from 40 to 50 kDa were observed from MCF-7 cytoplasmic proteins, while PC-3 showed a single cytoplasmic protein band. ^{125}I-labeled mAb H6-11 autoradiography (Figure 4B) confirmed that a single protein band was responsible for the immunoreactivity of mAb H6-11 to PC-3 versus the multiple protein bands, which were seen in MCF-7.

β-*N*-Acetylglucoside Glycosylation of H6-11 Antigen

To further explore the glycan type of H6-11 antigen epitope, we performed deglycosylation experiments. PC-3 cell lysates were digested with five different deglycosylation enzymes: *N*-glycanase PNGase F, sialidase A, *O*-glycanase, β(1–4) galactosidase, and β-*N*-

NIH-PA Author Manuscript

NIH-PA Author Manuscript

NIH-PA Author Manuscript

acetylglucosaminidase and then subjected to western blot analysis using ^{125}I-labeled mAb H6-11; gels were analyzed by autoradiography. The untreated lysate showed a clear band around 50 kDa; deglycosylation enzyme treatments using either *N*-glycanase PNGase F or sialidase A generated no significant changes (Figure 4C). When the cell lysate was treated with O-glycanase or β(1–4) galactosidase, the intensity of the 50 kDa band was slightly decreased, suggesting that the antigen epitope glycan is O-linked, rather than N-linked. When the PC-3 cell lysate was treated with β-*N*-acetylglucosaminidase (*O*-GlcNAc), the 50 kDa band disappeared (Figure 4C) suggesting that the *O*-GlcNAc is the main glycosylation structure of the H6-11 antigenic epitope.

In Vivo Optical Imaging of H6-11 Labeled with NIR Dye

A number of *O*-GlcNAc modified targets have been associated with various cancer types.[38–41] Recent studies suggested that *O*-GlcNAc transferase is overexpressed in prostate cancer compared with that in normal prostate epithelium.[39,42] The novel mAb H6-11 specifically recognized *O*-GlcNAc antigens; thus, we hypothesized that H6-11 would be a good imaging agent for prostate cancer. Therefore, we labeled mAb H6-11 with IRDye 800CW and conducted NIR imaging studies to determine the biodistribution and kinetic changes of the H6-11-IRDye 800CW conjugate in PC-3 tumor-bearing nude mice. As demonstrated in Figure 5A, the bilateral tumors were clearly visible 24 h postinjection. The fluorescence intensity of the tumor region was highest 48 h postinjection. The rapid clearance from nontarget regions and accumulation of this imaging probe in the xenograft prostate tumors resulted in high quality images, with good contrast even 120 h postinjection (Figure 5A).

MicroPET Studies

Because of the promising results of optical imaging, we decided to continue our exploration of *in vivo* imaging using microPET. Optical imaging is limited to shallow surface tissues due to the low penetration of fluorescent signals; thus, PET is a preferred modality for clinical studies. The novel mAb H6-11 was successfully conjugated with the chelator *p*-SCN-Bz-DFO and labeled with ^{89}Zr in 97% radiochemical yield. Both heavy and light chains showed ^{89}Zr labeling (Supporting Information, Figure S4). Chelation with *p*-SCN-Bz-DFO did not alter the immunoreactivity of H6-11 (Supporting Information, Figure S5). At different time points postinjection of ^{89}Zr–H6-11, static microPET scans were performed. Quantitative analysis of the images showed that the uptake gradually increased in the tumor tissue and decreased in the liver and heart until 48–72 h (Figure 5B). The tumor signal persisted at least 120 h postinjection (Figure 5B). This result was consistent with the optical imaging studies. In addition, microPET imaging showed that uptake was limited to the outer regions of the tumor; the tracer did not penetrate to the center of the solid tumor which suggests that *in vivo* tracer uptake may reflect differences in the tumor microenvironment (Figure 5B). The center area of the tumor was confirmed by histology as necrotic tumor tissue.[43,44] Similar phenomena have been reported previously.[43–46]

NIH-PA Author Manuscript

NIH-PA Author Manuscript

NIH-PA Author Manuscript

DISCUSSION

One of the most common changes in glycosylation for cancer cells is an increase in the side branching of N-linked or O-linked glycans.[42,47,48] This increased branching creates additional sites for terminal sialic acid residues, which, in combination with an up-regulation of sialyltransferases, leads to an increase in global sialylation, which is commonly associated with cancer development and progression. Glycosyl transferases (e.g., sialyl transferases and fucosyl transferases) involved in adding terminating residues to glycan tend to be overexpressed in breast cancer and prostate cancer.[37] The increased activity of these glycosyl transferases leads to an increase in certain terminal glycans. Glycan residues commonly found on transformed cells include sialyl Lewis^X, sialyl Tn, Globo-H, and polysialic acid. Many of these glycans have been observed in malignant cancer tissues.[2,13,15,37,49]

The addition of *O*-glycosidic GlcNAc in β linkage to Ser/Thr residues (*O*-GlcNAc) is a dynamic post-translational modification that occurs on numerous cytoplasmic and nuclear proteins and is distinct from complex carbohydrate synthesis in the secretory pathway.[42] Previous studies suggested that altered *O*-GlcNAcylation may play an important role in the pathogenesis of diabetes mellitus,[50,51] etiology of Alzheimer's disease,[50–52] and breast cancer development.[38,40,53] Recent studies suggested that *O*-GlcNAc modification is elevated in prostate cancer due to the overexpression of *O*-GlcNAc transferase in prostate cancer compared to that in normal prostate epithelium.[39,42] In this study, we found that the novel mAb H6-11 detected 95% of the prostate adenocarcinomas in a tissue array and specifically bound to the PC-3 human prostate cancer cell line. H6-11 also showed stronger immunostaining in PC-3 tumor xenografts than in the surrounding muscle (Figure 2). Subsequent *in vivo* optical and microPET imaging of PC-3 tumor-bearing nude mice confirmed that H6-11 was retained in the tumor and washed out of the muscle (Figure 5). These results are consistent with previous publications that *O*-GlcNAc glycosylation modification occurs more frequently in tumors than in normal muscle tissue.[42,47,48]

Biochemical analysis of the cytoplasm of different cell lines revealed that the antigen from the cytoplasm of PC-3 cells is a soluble glycoprotein with molecular weight ~50 kDa (Figure 4). The glycosylation of this antigen was confirmed to be *O*-GlcNAc (Figure 4C). Since both the breast cancer cell MCF-7 and the colon cancer cell line NSY42129 showed a positive reaction to H6-11 (Figure 4 and Supporting Information, Figure S2), and the epithelial cells from healthy prostate tissues also showed positive staining with H6-11 (Supporting Information, Table S1), we determined that the antigen recognized by H6-11 is not specific to prostate cancer. When we radiolabeled H6-11 with NIR dye and ^{89}Zr for *in vivo* imaging, our results in PC-3 tumor-bearing mice suggested that the *O*-GlcNAc-specific antibody (such as H6-11) is a good candidate for a cancer imaging agent because it showed good discrimination between tumor and normal tissues.

Cell surface antigens are easily accessible for binding to ligands including antibodies for tumor-targeted imaging and therapy. The binding of mAb H6-11 to living (cultured) cells indicates that the epitope recognized by the antibody is localized on cell membranes because living cells only allow surface molecules to be detected in immunofluorescent staining.

NIH-PA Author Manuscript

NIH-PA Author Manuscript

NIH-PA Author Manuscript

When the PC-3 cells were stained after fixation, the cytoplasmic antigens also showed a strong green fluorescent signal indicating that the *O*-GlcNAc-modified glycoprotein antigens are present not only on the surface of the tumor cells but also in the cytoplasm (Figure 2). This observation is consistent with the ~50 kDa band, which was clearly visualized by western blot analysis of soluble cytoplasmic proteins (Figure 4). Further mass spectrometry characterization of this unknown protein is underway, and may identify a new *O*-GlcNAc-modified antigen which binds to prostate and other cancers.

A major motivation for identifying tumor-specific ligands is to improve the diagnosis and treatment of cancer. Preclinical evaluation of imaging and therapeutic agents in animal models is a critical step for developing biological reagents for future clinical use. In tumor (n = 40) and normal tissue (n = 8) array analysis, the novel mAb H6-11 bound to ~95% of 40 different human prostate cancer tissue samples representing different disease stages or grades (Supporting Information, Figure S1). Although strong positive staining was observed, there was no positive correlation between disease stage and the staining intensity (Supporting Information, Figure S1). Normal prostate fibromuscular stroma showed negative mAb H6-11 staining (Figure 1). These results imply that mAb H6-11 is a good candidate for developing a biological imaging agent for the detection of prostate cancer or monitoring response to therapy. In this study, we observed that the probes accumulate in the tumor within 24 h postinjection and were retained in the tumor for at least 120 h.

We found that once an imaging probe is taken up in the xenograft prostate tumor, it accumulates and is retained during the period of washout from normal organs and tissues including the liver and kidney (Figure 5). H6-11-based imaging and therapeutic agents may be capable of detecting subclinical tumors *in vivo* and efficiently delivering anticancer drugs to the tumor cells. Conjugates of antibodies with imaging agents generally have high binding affinity and specificity. They are also retained in the tumor for a much longer time than smaller peptide-based imaging and therapeutic agents. An inherent disadvantage is that more time is required for clearance from normal tissues and organs. There are also concerns about the diffusion of antibody-based imaging and therapeutic reagents into deep tumor tissues where there is a higher interstitial fluid pressure and heterogeneous blood supply. Our microPET studies suggest that hypoxia or necrotic tissues prevent probe accumulation (Figure 5). This may limit the application of H6-11 for tumor imaging. Currently, we have sequenced the cDNA of the hybridoma cell line for H6-11 (Supporting Information, Figure S6); we can optimize the binding properties by antibody engineering as previously reported by other groups to improve tumor image quality.[54–56] Furthermore, mAb H6-11 conjugated with NIR fluorophores could be used to identify small masses associated with subclinical metastatic disease in the peritoneal region before and during surgery. Many prostate cancer patients (including Stage I patients) have unsuspected subclinical metastasis. Identifying subclinical tumors will help the physician to properly manage the disease and improve patient survival.

In summary, we characterized a novel mAb, H6-11, that specifically recognizes a ~50 kDa *O*-GlcNAc-modified glycoprotein found in PC-3 cancer cells. The K_d and B_{max} values measured for the ^{125}I-labled novel mAb with PC-3 tumor cells were similar to the values determined for Globo-H and MCF-7 cells, indicating that H6-11 displays typical antibody–

NIH-PA Author Manuscript

NIH-PA Author Manuscript

NIH-PA Author Manuscript

antigen binding. Molecular imaging techniques with two different H6-11 probes demonstrated good tumor to muscle contrast in PC-3 tumor-bearing nude mice using both NIR fluorescence and microPET imaging. This data collectively supports future studies on the application of a TACA-recognizing monoclonal antibody such as H6-11 for prostate tumor detection and imaging.

Supplementary Material

Refer to Web version on PubMed Central for supplementary material.

Acknowledgments

We appreciate the radionuclide production by the cyclotron facility at Washington University in St. Louis. We thank Nicole Fettig, Amanda Roth, Lori Strong, and Margaret Morris for their technical help and also Small Animal Imaging Facility of Washington University in St. Louis. We also appreciate Baogang Xu for the helpful discussions regarding the iodination experiment. We thank Lynne Jones for editing assistance. Experimental support was also provided by the Hybridoma Facility of the Rheumatic Diseases Core Center (NIH P03AR048335). Grant support: US Department of Defense, BCRP Award W81XWH-10-1-0031; and NIH grants R01 NS 075527 and R21 MH 092797.

ABBREVIATIONS

CT	computed tomography
CDR	complementarity-determining regions
DTPA	diethylenetriamine pentaacetic acid
FCS	fetal calf serum
HE	human epididymis
h	hour
i.v.	intravenous injection
i.p.	intraperitoneal injection
kDa	kilodalton
mAb	monoclonal antibody
NIR	near-infrared
***O*-GlcNAc**	O-linked β-*N*-acetylglucosamine
***p*-SCN-Bz-DFO**	*p*-isothiocyanatobenzyl-desferrioxamine
PBS	phosphate buffered saline
PEG	polyethylene glycol
PSL	photostimulated luminescence
PET	positron emission tomography
SPECT	single photon emission computed tomography
SDS–PAGE	sodium dodecyl sulfate–polyacrylamide gel electrophoresis

NIH-PA Author Manuscript

NIH-PA Author Manuscript

NIH-PA Author Manuscript

TACA	tumor-associated carbohydrate antigen
TLC	thin layer chromatography

REFERENCES

1. Tesarova P, Kalousova M, Trnkova B, Soukupova J, Argalasova S, Mestek O, Petruzelka L, Zima T. Carbonyl and oxidative stress in patients with breast cancer–is there a relation to the stage of the disease? Neoplasma. 2007; 54(3):219–224. [PubMed: 17447853]
2. Kumar SR, Sauter ER, Quinn TP, Deutscher SL. Thomsen-Friedenreich and Tn antigens in nipple fluid: Carbohydrate biomarkers for breast cancer detection. Clin. Cancer Res. 2005; 11(19 Pt 1): 6868–6871. [PubMed: 16203776]
3. Glinskii OV, Sud S, Mossine VV, Mawhinney TP, Anthony DC, Glinsky GV, Pienta KJ, Glinsky VV. Inhibition of prostate cancer bone metastasis by synthetic TF antigen mimic/galectin-3 inhibitor lactulose-L-leucine. Neoplasia (New York, NY). 2012; 14(1):65–73.
4. Khabaz MN, McClure J, McClure S, Stoddart RW. Glycophenotype of prostatic carcinomas. Folia Histochem. Cytobiol. 2010; 48(4):637–645. [PubMed: 21478109]
5. Mariano A, Di Carlo A, Santonastaso C, Oliva A, D'Armiento M, Macchia V. Expression of Lewis carbohydrate antigens and chromogranin A in human prostatic cancer. Int. J. Oncol. 2000; 17(1): 167–171. [PubMed: 10853035]
6. Marczynska A, Kulpa J, Lenko J, Bugajski A, Wojcik E. CA-50 serum level in patients with prostate cancer. Urol. Res. 1990; 18(3):189–191. [PubMed: 1697710]
7. Abel PD, Cornell C, Buamah PK, Williams G. Assessment of serum CA 19.9 as a tumour marker in patients with carcinoma of the bladder and prostate. Br. J. Urol. 1987; 59(5):427–429. [PubMed: 3474046]
8. Moore LE, Pfeiffer RM, Zhang Z, Lu KH, Fung ET, Bast RC Jr. Proteomic biomarkers in combination with CA 125 for detection of epithelial ovarian cancer using prediagnostic serum samples from the Prostate, Lung, Colorectal, and Ovarian (PLCO) Cancer Screening Trial. Cancer. 2012; 118(1):91–100. [PubMed: 21717433]
9. Xu M, Yuan Y, Xia Y, Achilefu S. Monoclonal antibody CC188 binds a carbohydrate epitope expressed on the surface of both colorectal cancer stem cells and their differentiated progeny. Clin. Cancer Res. 2008; 14(22):7461–7469. [PubMed: 19010863]
10. Bergeron A, LaRue H, Fradet Y. Biochemical analysis of a bladder-cancer-associated mucin: Structural features and epitope characterization. Biochem. J. 1997; 321(Pt 3):889–895. [PubMed: 9032480]
11. Li Q, Anver MR, Butcher DO, Gildersleeve JC. Resolving conflicting data on expression of the Tn antigen and implications for clinical trials with cancer vaccines. Mol. Cancer Ther. 2009; 8(4): 971–979. [PubMed: 19372570]
12. Slovin SF, Ragupathi G, Musselli C, Fernandez C, Diani M, Verbel D, Danishefsky S, Livingston P, Scher HI. Thomsen-Friedenreich (TF) antigen as a target for prostate cancer vaccine: Clinical trial results with TF cluster (c)-KLH plus QS21 conjugate vaccine in patients with biochemically relapsed prostate cancer. Cancer Immunol. Immunother. 2005; 54(7):694–702. [PubMed: 15726361]
13. Martensson S, Bigler SA, Brown M, Lange PH, Brawer MK, Hakomori S. Sialyl-Lewis^x and related carbohydrate antigens in the prostate. Hum. Pathol. 1995; 26(7):735–739. [PubMed: 7628844]
14. Wang CC, Huang YL, Ren CT, Lin CW, Hung JT, Yu JC, Yu AL, Wu CY, Wong CH. Glycan microarray of Globo H and related structures for quantitative analysis of breast cancer. Proc Natl Acad Sci U S A. 2008; 105(33):11661–11666. [PubMed: 18689688]
15. Chang WW, Lee CH, Lee P, Lin J, Hsu CW, Hung JT, Lin JJ, Yu JC, Shao LE, Yu J, Wong CH, Yu AL. Expression of Globo H and SSEA3 in breast cancer stem cells and the involvement of fucosyl transferases 1 and 2 in Globo H synthesis. Proc. Natl. Acad. Sci. U.S.A. 2008; 105(33): 11667–11672. [PubMed: 18685093]

NIH-PA Author Manuscript NIH-PA Author Manuscript NIH-PA Author Manuscript

16. Gilewski T, Ragupathi G, Bhuta S, Williams LJ, Musselli C, Zhang XF, Bornmann WG, Spassova M, Bencsath KP, Panageas KS, Chin J, Hudis CA, Norton L, Houghton AN, Livingston PO, Danishefsky SJ. Immunization of metastatic breast cancer patients with a fully synthetic globo H conjugate: A phase I trial. Proc. Natl. Acad. Sci. U.S.A. 2001; 98(6):3270–3275. [PubMed: 11248068]

17. LaRue H, Parent-Vaugeois C, Bergeron A, Champetier S, Fradet Y. Influence of spatial configuration on the expression of carcinoembryonic antigen and mucin antigens in human bladder cancer. Int. J. Cancer. 1997; 71(6):986–992. [PubMed: 9185702]

18. Xu M, Rettig MP, Sudlow G, Wang B, Akers WJ, Cao D, Mutch DG, DiPersio JF, Achilefu S. Preclinical evaluation of Mab CC188 for ovarian cancer imaging. Int. J. Cancer. 2012; 131(6): 1351–1359. [PubMed: 22130973]

19. Urban N, Thorpe JD, Bergan LA, Forrest RM, Kampani AV, Scholler N, O'Briant KC, Anderson GL, Cramer DW, Berg CD, McIntosh MW, Hartge P, Drescher CW. Potential role of HE4 in multimodal screening for epithelial ovarian cancer. J. Natl. Cancer Inst. 2011; 103(21):1630–1634. [PubMed: 21917606]

20. Donadio AC, Lobo C, Tosina M, de la Rosa V, Martin-Rufian M, Campos-Sandoval JA, Mates JM, Marquez J, Alonso FJ, Segura JA. Antisense glutaminase inhibition modifies the O-GlcNAc pattern and flux through the hexosamine pathway in breast cancer cells. J. Cell Biochem. 2008; 103(3):800–811. [PubMed: 17614351]

21. Havaki S, Kittas C, Marinos E, Dafni U, Sotiropoulou C, Voloudakis-Baltatzis I, Goutas N, Vassilaros SD, Athanasiou E, Arvanitis DL. Ultrastructural immunostaining of infiltrating ductal breast carcinomas with the monoclonal antibody H: A comparative study with cytokeratin 8. Ultrastruct. Pathol. 2003; 27(6):393–407. [PubMed: 14660278]

22. Firpo MA, Gay DZ, Granger SR, Scaife CL, DiSario JA, Boucher KM, Mulvihill SJ. Improved diagnosis of pancreatic adenocarcinoma using haptoglobin and serum amyloid A in a panel screen. World J. Surg. 2009; 33(4):716–722. [PubMed: 19082654]

23. Zhang Z, Yu Y, Xu F, Berchuck A, van Haaften-Day C, Havrilesky LJ, de Bruijn HW, van der Zee AG, Woolas RP, Jacobs IJ, Skates S, Chan DW, Bast RC Jr. Combining multiple serum tumor markers improves detection of stage I epithelial ovarian cancer. Gynecol. Oncol. 2007; 107(3): 526–531. [PubMed: 17920110]

24. Chaturvedi R, Heimburg J, Yan J, Koury S, Sajjad M, Abdel-Nabi HH, Rittenhouse-Olson K. Tumor immunolocalization using ^{124}I-iodine-labeled JAA-F11 antibody to Thomsen-Friedenreich alpha-linked antigen. Appl. Radiat. Isot. 2008; 66(3):278–287. [PubMed: 17890096]

25. Lieberman G, Buscombe JR, Hilson AJ, Reid WM, Thakrar D, Maclean AB. Preoperative diagnosis of ovarian carcinoma with a novel monoclonal antibody. Am. J. Obstet. Gynecol. 2000; 183(3):534–540. [PubMed: 10992170]

26. Tibben JG, Massuger LF, Claessens RA, Schijf CP, Pak KY, Strijk SP, Kenemans P, Corstens FH. Tumour detection and localization using ^{99m}Tc-labelled OV-TL 3 Fab' in patients suspected of ovarian cancer. Nucl. Med. Commun. 1992; 13(12):885–893. [PubMed: 1465272]

27. Xu M, Wright WD, Higashikubo R, Roti JL. Chronic thermotolerance with continued cell proliferation. Int. J. Hyperthermia. 1996; 12(5):645–660. discussion 661–662.. [PubMed: 8886891]

28. Thean ET, Toh BH. Production and characterization of murine monoclonal antibody to human alpha-lactalbumin. Immunol. Cell Biol. 1989; 67(Pt 1):41–48. [PubMed: 2722208]

29. Mandeville R, Dumas F, Amarouch A, Sidrac-Ghali S, Walker MC, Zelechowska M, Ajdukovic I, Grouix B. Affinity purification of a high molecular weight human breast cancer-associated antigen identified by the BCD-B4 monoclonal antibody. Hybridoma. 1987; 6(5):441–451. [PubMed: 3679257]

30. Xu M, Wang F, Gildersleeve JC, Achilefu S. MAb L9E10 to blood group H2 antigen binds to colon cancer stem cells and inhibits tumor cell migration and invasion. Hybridoma. 2010; 29(4): 355–359. [PubMed: 20715995]

31. Jadvar H, Xiankui L, Shahinian A, Park R, Tohme M, Pinski J, Conti PS. Glucose metabolism of human prostate cancer mouse xenografts. Mol. Imaging. 2005; 4(2):91–97. [PubMed: 16105512]

NIH-PA Author Manuscript

NIH-PA Author Manuscript

NIH-PA Author Manuscript

32. Zheng QH, Gardner TA, Raikwar S, Kao C, Stone KL, Martinez TD, Mock BH, Fei X, Wang JQ, Hutchins GD. [^{11}C]Choline as a PET biomarker for assessment of prostate cancer tumor models. Bioorg. Med. Chem. 2004; 12(11):2887–2893. [PubMed: 15142549]
33. Vosjan MJWD, Perk LR, Visser GWM, Budde M, Jurek P, Kiefer GE, van Dongen GAMS. Conjugation and radiolabeling of monoclonal antibodies with zirconium-89 for PET imaging using the bifunctional chelate p-isothiocyanatobenzyl-desferrioxamine. Nat. Protoc. 2010; 5(4):739–743. [PubMed: 20360768]
34. Perk LR, Vosjan MJWD, Visser GWM, Budde M, Jurek P, Kiefer GE, van Dongen GAMS. p-Isothiocyanatobenzyl-desferrioxamine: A new bifunctional chelate for facile radiolabeling of monoclonal antibodies with zirconium-89 for immuno-PET imaging. Eur. J. Nucl. Med. Mol. Imaging. 2010; 37(2):250–259. [PubMed: 19763566]
35. Pu Y, Wang WB, Xu M, Tang GC, Budansky Y, Sharanov M, Achilefu S, Eastham JA, Alfano RR. Near infrared photonic finger imager for prostate cancer screening. Technol. Cancer Res. Treat. 2011; 10(6):507–517. [PubMed: 22066592]
36. Girgis MD, Kenanova V, Olafsen T, McCabe KE, Wu AM, Tomlinson JS. Anti-CA19-9 diabody as a PET imaging probe for pancreas cancer. J. Surg. Res. 2011; 170(2):169–178. [PubMed: 21601881]
37. Jin H, Zangar RC. Protein modifications as potential biomarkers in breast cancer. Biomarker Insights. 2009; 4:191–200. [PubMed: 20072669]
38. Rambaruth ND, Greenwell P, Dwek MV. The lectin Helix pomatia agglutinin recognizes O-GlcNAc containing glycoproteins in human breast cancer. Glycobiology. 2012; 22(6):839–848. [PubMed: 22322011]
39. Lynch TP, Ferrer CM, Jackson SR, Shahriari KS, Vosseller K, Reginato MJ. Critical role of O-Linked beta-N-acetylglucosamine transferase in prostate cancer invasion, angiogenesis, and metastasis. J. Biol. Chem. 2012; 287(14):11070–11081. [PubMed: 22275356]
40. Krzeslak A, Forma E, Bernaciak M, Romanowicz H, Brys M. Gene expression of O-GlcNAc cycling enzymes in human breast cancers. Clin. Exp. Med. 2012; 12(1):61–65. [PubMed: 21567137]
41. Mi W, Gu Y, Han C, Liu H, Fan Q, Zhang X, Cong Q, Yu W. O-GlcNAcylation is a novel regulator of lung and colon cancer malignancy. Biochim. Biophys. Acta. 2011; 1812(4):514–519. [PubMed: 21255644]
42. Sayat R, Leber B, Grubac V, Wiltshire L, Persad S. O-GlcNAc-glycosylation of beta-catenin regulates its nuclear localization and transcriptional activity. Exp. Cell Res. 2008; 314(15):2774–2787. [PubMed: 18586027]
43. Cho H, Ackerstaff E, Carlin S, Lupu ME, Wang Y, Rizwan A, O'Donoghue J, Ling CC, Humm JL, Zanzonico PB, Koutcher JA. Noninvasive multimodality imaging of the tumor microenvironment: registered dynamic magnetic resonance imaging and positron emission tomography studies of a preclinical tumor model of tumor hypoxia. Neoplasia. 2009; 11(3):247–259. 2p following 259.. [PubMed: 19242606]
44. Uehara H, Miyagawa T, Tjuvajev J, Joshi R, Beattie B, Oku T, Finn R, Blasberg R. Imaging experimental brain tumors with 1-aminocyclopentane carboxylic acid and alpha-aminoisobutyric acid: Comparison to fluorodeoxyglucose and diethylenetriaminepenta-acetic acid in morphologically defined tumor regions. J. Cereb. Blood Flow Metab. 1997; 17(11):1239–1253. [PubMed: 9390656]
45. Wakefield LM, Letterio JJ, Chen T, Danielpour D, Allison RS, Pai LH, Denicoff AM, Noone MH, Cowan KH, O'Shaughnessy JA, et al. Transforming growth factor-beta1 circulates in normal human plasma and is unchanged in advanced metastatic breast cancer. Clin. Cancer Res. 1995; 1(1):129–136. [PubMed: 9815895]
46. Apostolopoulos V, Xing PX, Trapani JA, McKenzie IF. Production of anti-breast cancer monoclonal antibodies using a glutathione-S-transferase-MUC1 bacterial fusion protein. Br. J. Cancer. 1993; 67(4):713–720. [PubMed: 7682431]
47. Samih N, Hovsepian S, Notel F, Prorok M, Zattara-Cannoni H, Mathieu S, Lombardo D, Fayet G, El-Battari A. The impact of N- and O-glycosylation on the functions of Glut-1 transporter in human thyroid anaplastic cells. Biochim. Biophys. Acta. 2003; 1621(1):92–101. [PubMed: 12667615]

NIH-PA Author Manuscript

NIH-PA Author Manuscript

NIH-PA Author Manuscript

48. Heffernan M, Lotan R, Amos B, Palcic M, Takano R, Dennis JW. Branching beta 1–6N-acetylglucosaminetransferases and polylactosamine expression in mouse F9 teratocarcinoma cells and differentiated counterparts. J. Biol. Chem. 1993; 268(2):1242–1251. [PubMed: 8419327]

49. MacLean GD, Reddish M, Koganty RR, Wong T, Gandhi S, Smolenski M, Samuel J, Nabholtz JM, Longenecker BM. Immunization of breast cancer patients using a synthetic sialyl-Tn glycoconjugate plus Detox adjuvant. Cancer Immunol. Immunother. 1993; 36(4):215–222. [PubMed: 8439984]

50. Li X, Lu F, Wang JZ, Gong CX. Concurrent alterations of O-GlcNAcylation and phosphorylation of tau in mouse brains during fasting. Eur. J. Neurosci. 2006; 23(8):2078–2086. [PubMed: 16630055]

51. Robertson LA, Moya KL, Breen KC. The potential role of tau protein O-glycosylation in Alzheimer's disease. J. Alzheimer's Dis. 2004; 6(5):489–495. [PubMed: 15505370]

52. Yao PJ, Coleman PD. Reduced O-glycosylated clathrin assembly protein AP180: Implication for synaptic vesicle recycling dysfunction in Alzheimer's disease. Neurosci. Lett. 1998; 252(1):33–36. [PubMed: 9756352]

53. Caldwell SA, Jackson SR, Shahriari KS, Lynch TP, Sethi G, Walker S, Vosseller K, Reginato MJ. Nutrient sensor O-GlcNAc transferase regulates breast cancer tumorigenesis through targeting of the oncogenic transcription factor FoxM1. Oncogene. 2010; 29(19):2831–2842. [PubMed: 20190804]

54. Olafsen T, Wu AM. Antibody vectors for imaging. Semin. Nucl. Med. 2010; 40(3):167–181. [PubMed: 20350626]

55. Wei LH, Olafsen T, Radu C, Hildebrandt IJ, McCoy MR, Phelps ME, Meares C, Wu AM, Czernin J, Weber WA. Engineered antibody fragments with infinite affinity as reporter genes for PET imaging. J. Nucl. Med. 2008; 49(11):1828–1835. [PubMed: 18927335]

56. Wu AM, Olafsen T. Antibodies for molecular imaging of cancer. Cancer J. (Sudbury, MA). 2008; 14(3):191–197.

NIH-PA Author Manuscript
NIH-PA Author Manuscript
NIH-PA Author Manuscript

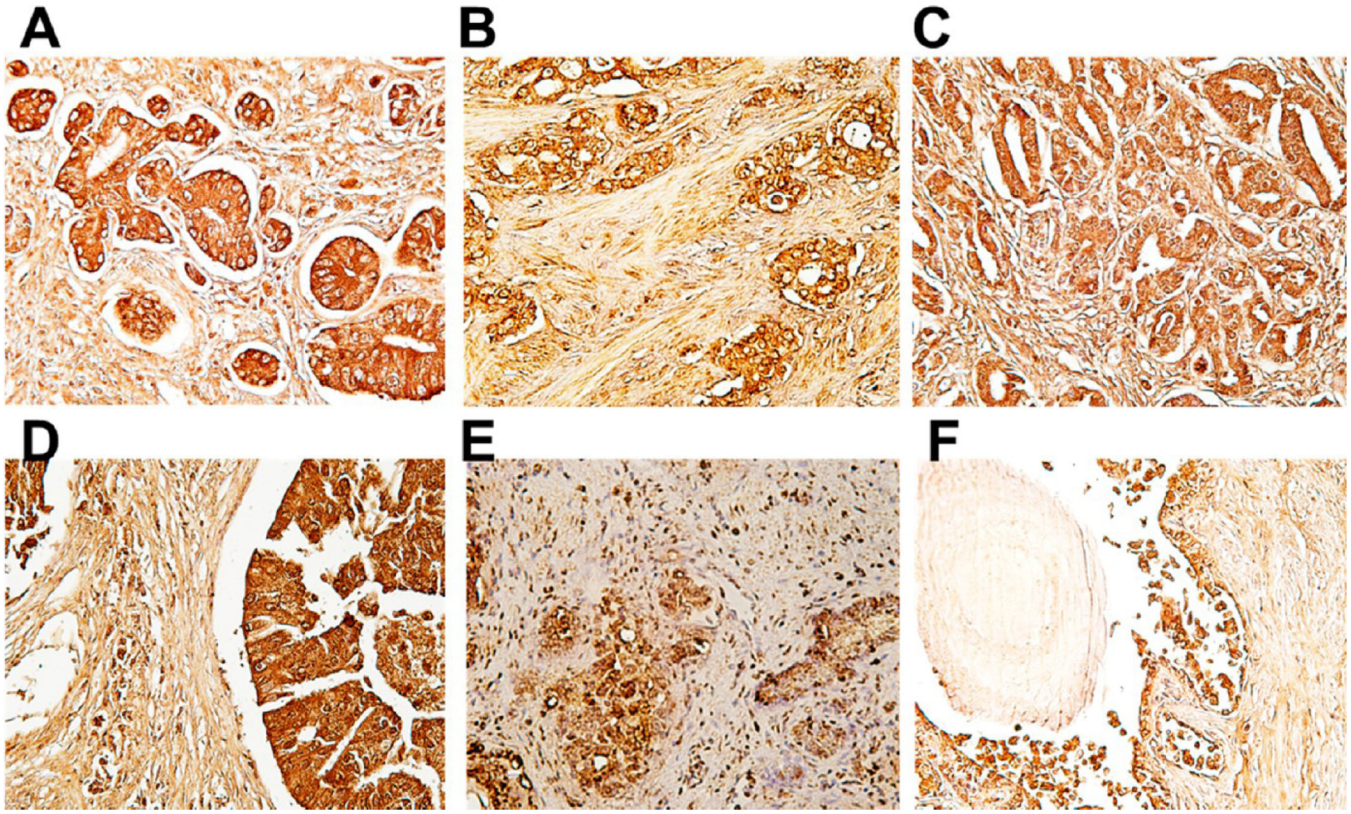

Figure 1.

Immunohistochemical staining of mAb H6-11 in different histological grades of prostate cancer (A–E) and in normal prostate tissues (F). (A–E) Different stages of prostate cancer tissues showed positive staining with H6-11. (F) Normal prostate stroma showed negative staining with mAb H6-11, while the prostate gland showed weak positives staining (+).

NIH-PA Author Manuscript
NIH-PA Author Manuscript
NIH-PA Author Manuscript

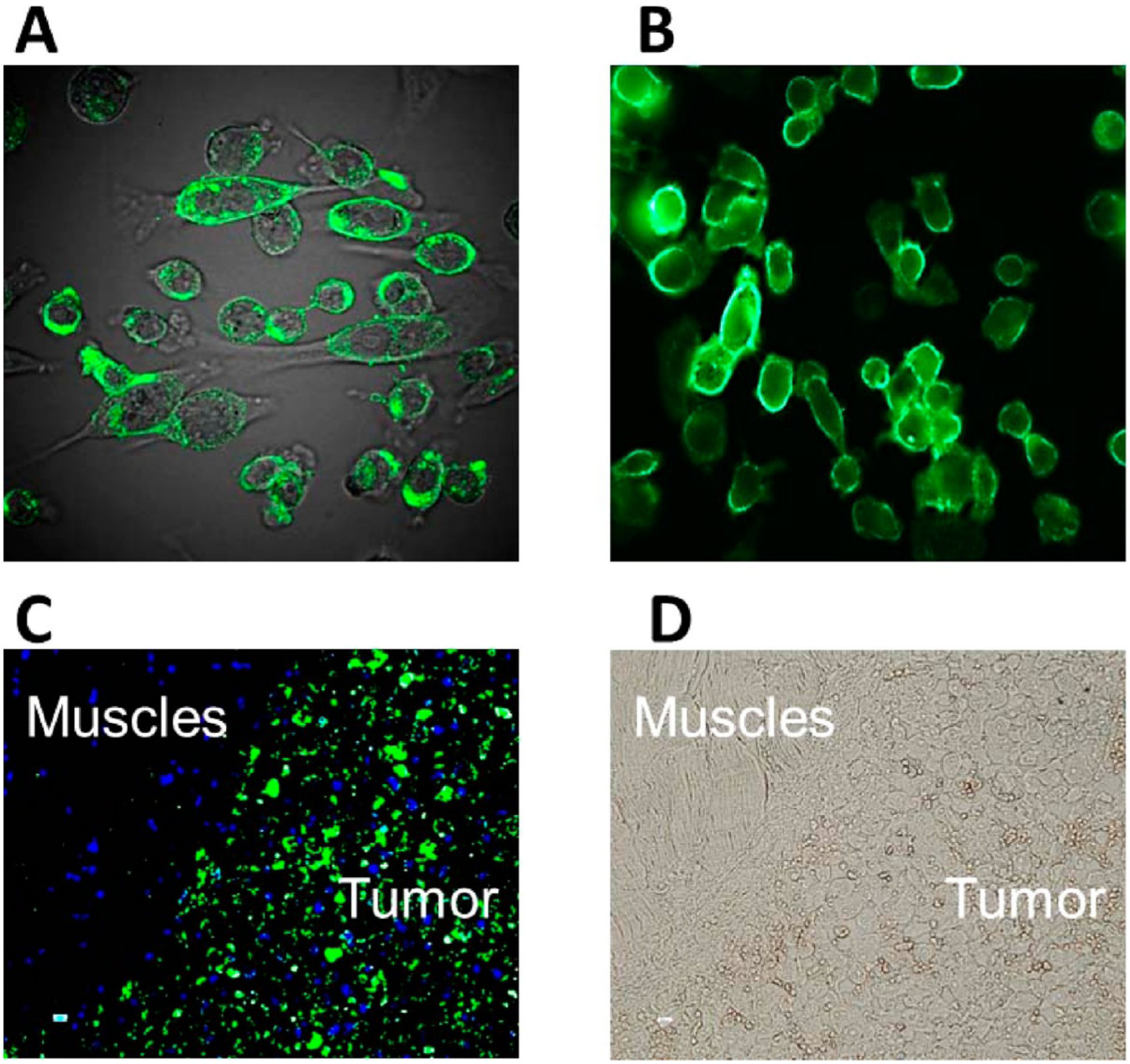

Figure 2.

mAb H6-11 immunofluorescence staining of the PC-3 prostate tumor cell line and of PC-3 solid tumor xenografts harvested from nude mice. (A) Human prostate cancer PC-3 cells were fixed with 10% neutral buffered formalin and then immunostained with H6-11. (B) Unfixed PC-3 cells were directly immunostained with H6-11. (C) Immunostaining of PC-3 solid tumors with H6-11. The blue color is the DPI staining for nucleic acid. (D) Bright field of panel C.

NIH-PA Author Manuscript
NIH-PA Author Manuscript
NIH-PA Author Manuscript

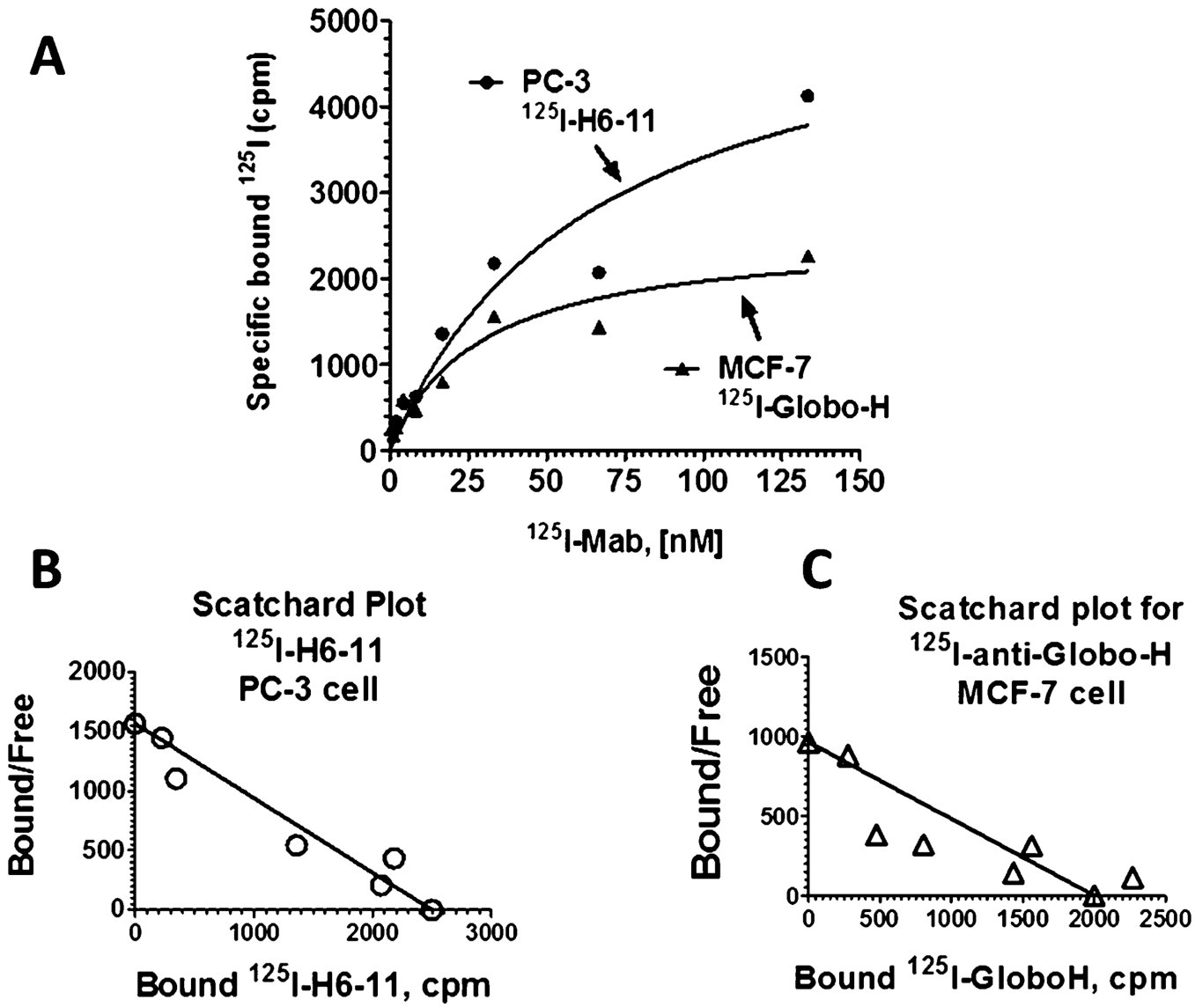

Figure 3.

Radioactive ligand saturation binding studies with ^{125}I-labeled H6-11. (A) Variable concentrations of ^{125}I–labeled H6-11 incubated with a constant number of PC-3 prostate cancer cells (●). As a positive control, variable concentrations of ^{125}I-anti-Globo-H antibody were incubated with a constant number of MCF-7 breast cancer cells (▲). (B) The B_{max} and K_d values were estimated from the Scatchard plot for the binding of ^{125}I–H6-11 to PC-3 cells, and (C) Scatchard plot for the binding of ^{125}I-anti-Globo-H antibody to breast cancer MCF-7 cells.

NIH-PA Author Manuscript
NIH-PA Author Manuscript
NIH-PA Author Manuscript

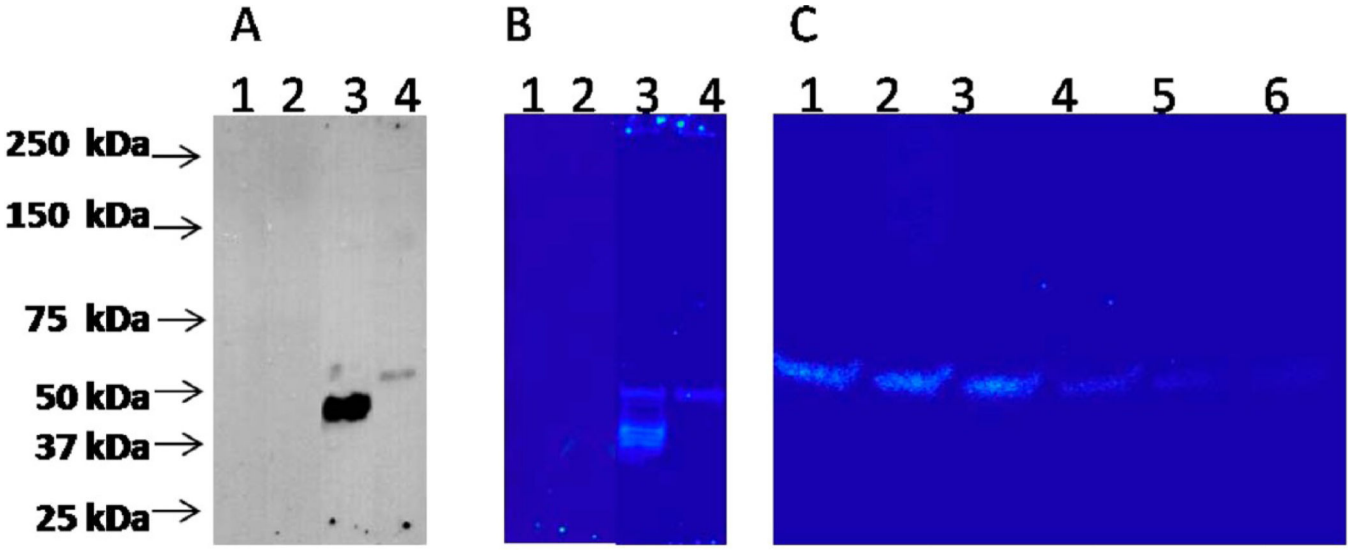

Figure 4.

O-GlcNAc is the main glycosylation structure of the H6-11 antigenic epitope. (A) Breast cancer cell line MCF-7 (lanes 1 and 3) and prostate cancer cell line PC-3 (lanes 2 and 4) were lysed and subjected to western blot analysis with anti-Globo-H antibody (lanes 1 and 2) and H6-11 (lanes 3 and 4) as the primary antibody and HRP-labeled anti mouse IgG as the secondary antibody. (B) Breast cancer cell line MCF-7 (lanes 1 and 3) and prostate cancer cell line PC-3 (lanes 2 and 4) were lysed and subjected to western blot analysis with ^{125}I-labeled anti-Globo-H antibody (lanes 1 and 2) and H6-11 (lanes 3 and 4), respectively. (C) PC-3 cell line lysate was digested with 5 different deglycosylation enzymes (lane 1, uncut control; lane 2, *N*-glycanase PNGase F; lane 3, sialidase A; lane 4, *O*-glycanase; lane 5, β(1–4) galactosidase; and lane 6, β-*N*-acetyl glucosaminidase) and subjected to western blot analysis using ^{125}I-labeled H6-11.

NIH-PA Author Manuscript

NIH-PA Author Manuscript

NIH-PA Author Manuscript

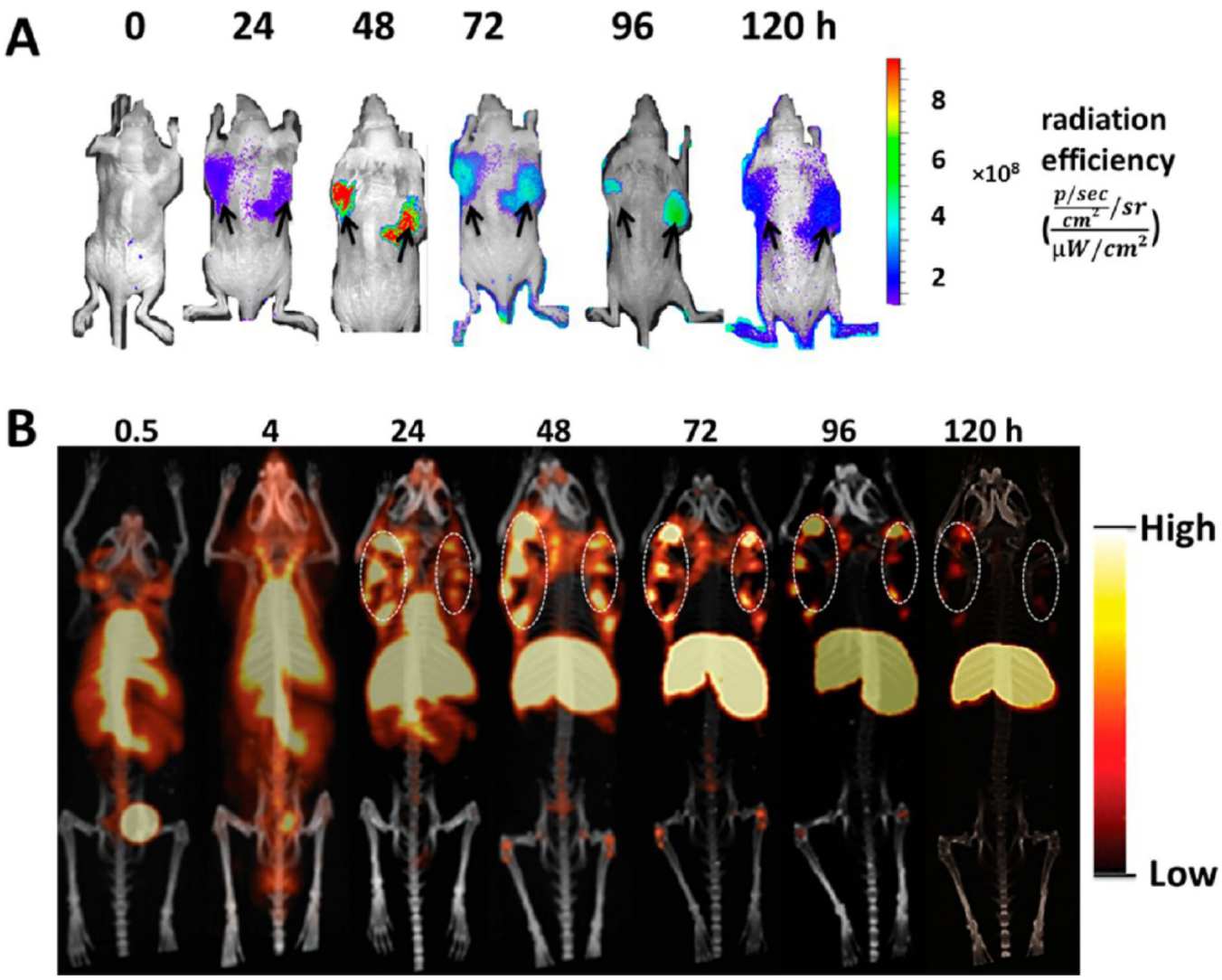

Figure 5.

In vivo molecular imaging of PC-3 tumor-bearing athymic mice. (A) H6-11-IRDye 800CW optical imaging of PC-3 tumor-bearing mice at 0, 24, 48, 72, 96, and 120 h postinjection. The maximum tumor uptake is around 48–72 h. The black arrows indicate the tumors. (B) ^{89}Zr-labeled H6-11 microPET coronal imaging of PC-3 tumor-bearing mice at 0.5, 4, 24, 48, 72, 96, and 120 h postinjection. The dashed white circles are the bilaterally implanted tumors. A scale bar is shown beside each image.